9 Mechanisms and Dynamics of Fluorescence Quenching

In the previous chapter we described the basic principles and biochemical applications of quenching. Quenching requires molecular contact between the fluorophore and quencher. This contact can be due to diffusive encounters, which is dynamic quenching, or due to complex formation, which is static quenching. Because of the close distance interaction required for quenching, the extent of quenching is sensitive to molecular factors that affect the rate and probability of contact, including steric shielding and charge–charge interactions. In contrast, resonance energy transfer is a through-space interaction that occurs over longer distances and is insensitive to these factors.

In this chapter we describe quenching in more detail. Initially we compare quenching with resonance energy transfer, which illustrates the different types of interactions for these two processes. We then describe the different types of chemical and/or electronic interactions that cause quenching. These interactions include intersystem crossing, electron exchange, and photoinduced electron transfer. Since quenching occurs over short distances, diffusion is needed for efficient quenching. This results in transient effects, which cause the intensity decays to become non-exponential. This effect can complicate interpretation of the time-resolved data, but also provide additional information about the distances and dynamics of quenching.

9.1. COMPARISON OF QUENCHING AND RESONANCE ENERGY TRANSFER

Any process that causes a decrease in intensity can be considered to be quenching. Quenching results in dissipation of the fluorophore's electronic energy as heat. Resonance energy transfer (RET) decreases the intensity of the donor and transfers the energy to an acceptor. The acceptor can be fluorescent or nonfluorescent, but in both cases the fluorescence intensity of the initially excited molecule is decreased. Comparison of RET and quenching clarifies the nature of both processes. Figure 9.1 shows a molecular orbital schematic for RET. The fluorophore initially has two electrons in the highest-occupied (HO) molecular orbital. Absorption of light results in elevation of one electron to the lowest-unoccupied (LU) orbital. When RET occurs the electron in the excited donor (D_R*) returns to the ground state. Simultaneously an electron in the acceptor (A_R) goes into a higher excited-state orbital. If the acceptor is fluorescent it may then emit. If the acceptor is nonfluorescent the energy is dissipated as heat. The mechanism of RET is the same whether the acceptor is fluorescent or nonfluorescent: simultaneous electron transitions in D_R and A_R. The subscript R refers to RET and will be used to distinguish RET from other mechanisms of quenching discussed in this chapter.

It is informative to consider the size of the fluorophores as compared to the distances for RET.[1–3] The donor and acceptor molecules in Figure 9.1 are drawn roughly to scale relative to the Förster distance R_0, which is the distance at which RET is 50% efficient. From comparison of the distance for RET with the size of the molecules, one can see that RET is a through-space interaction. The assumed Förster distance of 30 Å is too large for direct interaction between the electron clouds in the molecules. This schematic also shows that RET does not require molecular contact between D_R and A_R. For this reason RET is not sensitive to steric factors or electrostatic interactions.

Figure 9.2 shows a schematic for quenching, again drawn to scale. For quenching to occur the fluorophore (F) and quencher (Q) have to come into molecular contact, allowing the electron clouds of both molecules to interact.

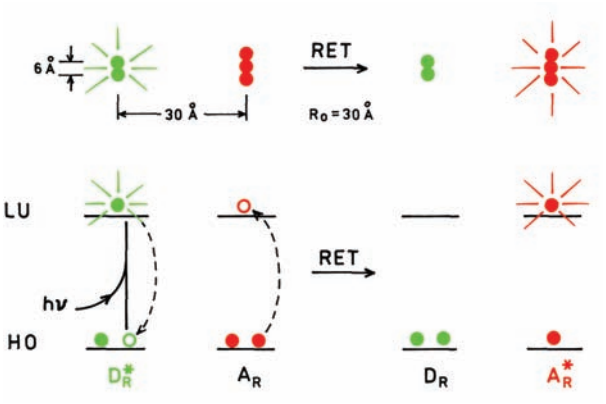

Figure 9.1. Molecular orbital schematic for resonance energy transfer. The top row shows the size of fluorophores relative to the Förster distance R_0.

The electron density falls off very rapidly with distance from the surface of the molecules, typically decreasing as $\exp[-\beta(r - r_c)]$ where $1/\beta$ is near 1 Å, r is the center-to-center distance, and r_c is the center-to-center distance upon molecular contact. This interaction becomes insignificant for distances r larger than several angstroms.

Because the electron clouds are strongly localized, quenching requires molecular contact at the van der Waals radii. When the quencher comes in contact with the excited fluorophore its excited electron in the LU orbital returns to the ground state. The fluorophore cannot emit, and the energy is dissipated as heat. In Figure 9.2 the quencher is shown as remaining in the ground state. Depending on the mechanism, this may occur or the quencher can also go to an excited state, which then returns to the ground state. The important point is that quenching is due to short-range interactions between F and Q, and RET is due to long-range

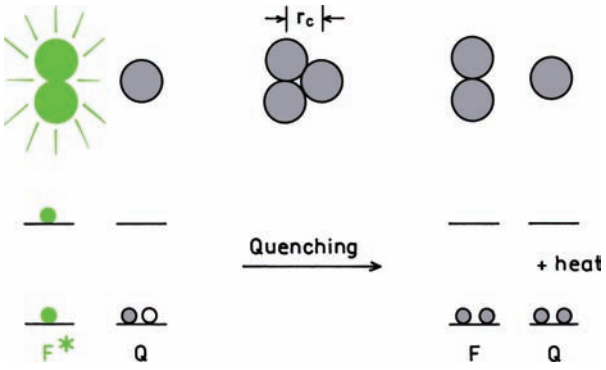

Figure 9.2. Schematic of fluorescence quenching.

dipolar interactions through D_R* and A_R. The different distance dependence of quenching and RET results in different molecular information being available from each phenomenon. The description of quenching in Figure 9.2 is purely phenomenological and does not consider the nature of the interaction between F* and Q.

9.1.1. Distance Dependence of RET and Quenching

It is informative to examine simulations on the distance dependence of RET and quenching between the molecules. The rate of energy transfer is given by

$$k_T(r) = \frac{1}{\tau_D}\left(\frac{R_0}{r}\right)^6 \tag{9.1}$$

where τ_D is the donor lifetime in the absence of acceptor, r is the center-to-center distance between D_R and A_R, and R_0 is the Förster distance.

The rate of quenching depends on the extent of interaction between the electron clouds in F and Q. Since the electron density decreases exponentially with distance from the nuclei, the rate of quenching depends on the distance according to

$$k_E(r) = A\,\exp\left[-\beta(r - r_c)\right] \tag{9.2}$$

where r is the center-to-center distance between F and Q, and r_c is the distance of closest approach at molecular contact. For interactions between orbitals, A is expected to have a value near 10^{13} s^{-1}. The values of β are typically near 1 $Å^{-1}$. These interactions between orbitals are usually called electron exchange (E) or exchange interactions because electrons can move between the molecules at these short distances. Equation 9.2 describes the quenching rate for a fluorophore and quencher at a distance r. This equation does not include the effect of diffusion on quenching.

Equations 9.1 and 9.2 can be used to show how RET and quenching depends on distance. Figure 9.3 shows simulated values for $k_T(r)$ and $k_E(r)$. For RET we assumed τ_D = 1 ns and R_0 = 30 Å. The rate of energy transfer remains high for distances of 20 Å or longer. The right-side axis shows the rate constant as the frequency of transfer events. For D_R and A_R at a distance of 20 Å, the frequency of events is about tenfold larger than the reciprocal lifetime or emission frequency. This shows that at 20 Å RET can occur about

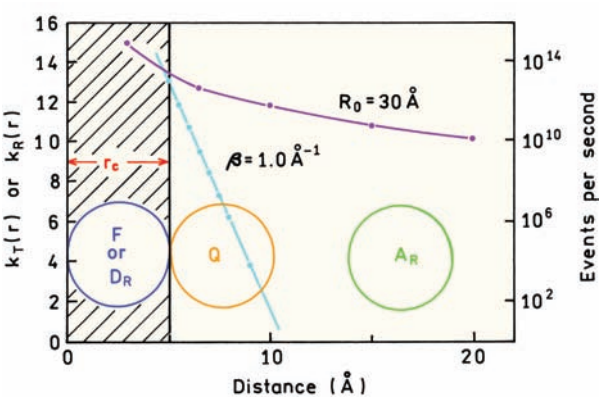

Figure 9.3. Distance-dependent rate constants for RET and exchange interactions. For these simulations τ_D = 1 ns, R_0 = 30Å, β = Å^{-1}, and r_c = 5 Å.

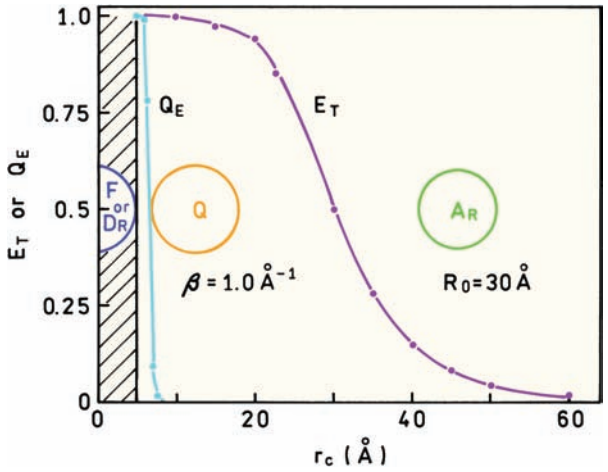

Figure 9.4. Calculated efficiencies for resonance energy transfer E_T and for quenching Q_E. The parameter values are the same as used in Figure 9.3.

tenfold faster than emission, and will thus be about 90% efficient.

The dependence on distance is remarkably different for electron exchange. The value of $k_E(r)$ drops rapidly with distance. When the nuclei are 10 Å apart, with r_c = 5 Å, the electron clouds are 5 Å apart. At this short distance, the exchange rate of 10^4 is much smaller than the emission rate of 10^9, so that essentially no exchange will occur during the 1 ns lifetime. When the distance between the electron clouds is less than 2 Å and r_c = 7 Å, the exchange rate has already decreased to less than the emission rate, so that the quenching is less than 100% efficient. This result shows that close molecular contact is needed for quenching.

Another way to compare RET and quenching is to consider the RET transfer efficiency E_T or the quenching efficiency Q_E (Figure 9.4). These efficiencies were calculated using the same parameter values as used in Figure 9.3. The RET efficiency can be calculated using

$$E_T = \frac{k_T(r)}{\gamma + k_T(r)} \tag{9.3}$$

where $\gamma = \tau_D^{-1}$ is the donor decay rate in the absence of acceptor. The quenching efficiency can be calculated using

$$Q_E = \frac{k_E(r)}{\gamma + k_E(r)} \tag{9.4}$$

These calculations show that RET is efficient over long distances, but quenching is efficient only at very short distances, when the electron clouds are within 2 Å. While eqs. 9.3 and 9.4 appear similar, there is an important difference. In eq. 9.3 the rate $k_T(r)$ contains a factor $\gamma = \tau_D^{-1}$, so that the RET efficiency is independent of the donor decay time. In eq. 9.4 the exchange rate $k_E(r)$ is independent of the fluorophore decay time. For this reason the quenching occurs over longer distances for longer decay time fluorophores. However, this effect is modest and very long lifetimes are needed to substantially increase the transfer distance.

9.1.2. Encounter Complexes and Quenching Efficiency

Unless the quencher concentrations are very high, significant quenching requires diffusion to bring the molecules into contact. Figure 9.5 shows a kinetic scheme for quenching. The molecules come in contact by the bimolecular rate constant k_0. Upon collision the molecules form an encounter complex. This complex can proceed to quenching with a rate constant $k(r)$, or break apart with a rate constant k_2. The efficiency of quenching is given by

$$E_Q = \frac{k(r)}{k_2 + k(r)} \tag{9.5}$$

Typically, $k(r)$ is much larger than k_2, so that each encounter results in quenching. Some authors consider the possibility of emission from the encounter complex, in which case an additional term, $\gamma = \tau_D^{-1}$, appears in the denominator of eq. 9.5.[4–5]

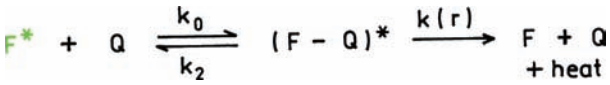

Figure 9.5. Kinetic scheme for quenching.

The concept of an encounter complex is clarified by considering the distances a quencher can diffuse during the excited state lifetime. The mean square distance is given by

$$\Delta x^2 = 2D\tau \tag{9.6}$$

where D is the diffusion coefficient and τ is the lifetime. Figure 9.6 illustrates how a quencher can diffuse over long distances. During 1 ns the quencher diffuses an average of 15 Å. During 100 ns the quencher diffuses an average of 150 Å. Since the quencher moves randomly one can see that a quencher will usually undergo many collisions with a fluorophore prior to diffusing away from the fluorophore. An encounter complex is thus a fluorophore and quencher in close proximity, probably with one or no intervening solvent molecules.

The concept of an encounter complex shows how the quenching efficiency can depend on viscosity. If quenching is efficient, each encounter results in quenching. However, if quenching is inefficient then the pair may diffuse apart prior to quenching. In this case the quenching efficiency will be higher at higher viscosities because F* and Q remain close together for a longer period of time, allowing more time for quenching to occur.

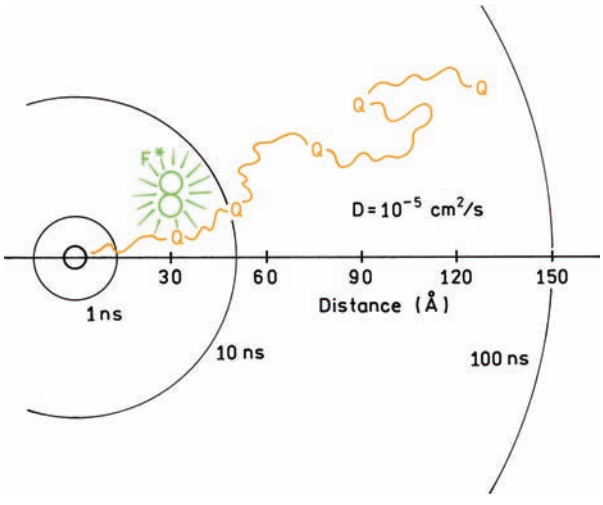

Figure 9.6. Distances for diffusion for various times. $D = 10^{-5}$ cm^2/s.

9.2. MECHANISMS OF QUENCHING

Equation 9.2 describes the effect of distance on quenching, but does not reveal the mechanism of quenching. There are at least three mechanisms for quenching:

1. Intersystem crossing or the heavy atom effect
2. Electron exchange or Dexter interactions
3. Photoinduced electron transfer

All of these mechanisms are expected to have the same distance dependence described by eq. 9.2. It is often difficult to know the mechanism of quenching. The mechanisms are not mutually exclusive, and many reports indicate that quenching occurs by a combination of these mechanisms. We will use these three mechanisms as limiting cases to provide a framework of discussion.

9.2.1. Intersystem Crossing

Quenching by heavy atoms halogens[6–14] and oxygen[15] is thought to occur by intersystem crossing. An encounter with a heavy atom or a triplet oxygen molecule is thought to cause the excited singlet state to become an excited triplet (Figure 9.7). Since the triplet states are usually long lived and also quenched by oxygen,[16–17] they are likely to be quenched to the ground state by the same quencher, or return to the ground state by non-radiative decay. It is not always clear which mechanism is dominant. Various reports have suggested oxygen quenching occurs by mixed mechanisms that include intersystem crossing, charge transfer, and electron exchange.[18–20] Depending upon the structure of the fluorophore, quenching by halogens has also been

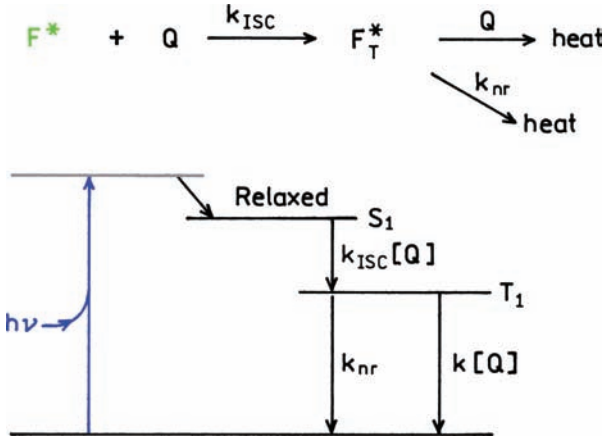

Figure 9.7. Quenching by intersystem crossing.

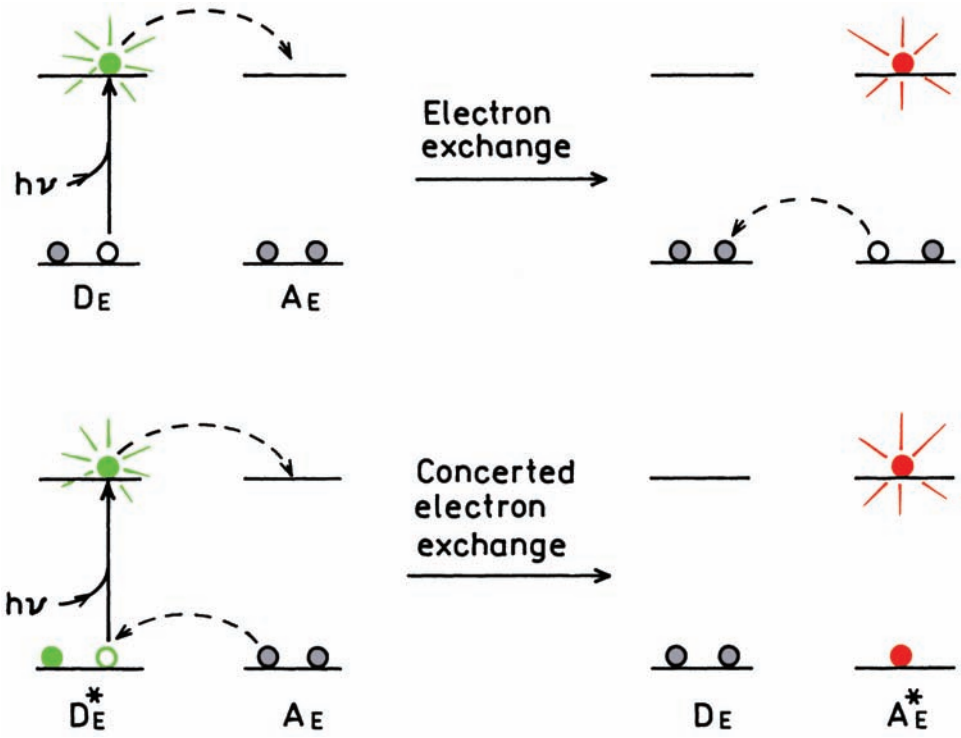

Figure 9.8. Schematic for stepwise (top) or concerted (bottom) electron exchange.

attributed to charge transfer, intersystem crossing, and/or electron exchange.[21–30] In general it seems that halocarbons quench by intersystem crossing and halides quench by charge transfer. Additionally, many fluorophores undergo photodestruction in the presence of halocarbons.[31–33]

9.2.2. Electron-Exchange Quenching

Figure 9.8 shows a schematic for the electron exchange or Dexter interaction.[34–37] This interaction occurs between a donor D_E and an acceptor A_E, where E indicates electron exchange. The excited donor has an electron in the LU orbital. This electron is transfer to the acceptor. The acceptor then transfers an electron back to the donor. This electron comes from the HO orbital of the acceptor, so the acceptor is left in an excited state. Electron exchange is similar to RET because energy is transferred to an acceptor. This mode of energy transfer also depends on spectral overlap of the donor and acceptor, just like RET. In contrast to RET, the Dexter interaction is a quantum mechanical effect that does not have an analogy in classical electrodynamics.

RET is well known to result in an excited acceptor. In contrast, the Dexter interaction is usually associated with quenching. This association occurs because RET occurs over large distances, so if there is spectral overlap the transfer occurs by RET before Dexter transfer can occur. Dexter transfer may occur at short donor–acceptor distances, but the donor will be completely quenched by RET or Dexter transfer, and thus non-observable. Dexter transfer can be observed if the spectral overlap is small, so that the large rates of exchange become significant. Additionally, high concentrations are needed for significant Dexter transfer, whereas RET occurs at much lower concentrations. For an unlinked donor and acceptor the bulk concentration of the acceptor needs to be about 10^{-2} M to have an average distance of 30 Å. For a fluorophore and quencher the bulk quencher concentration needs to be near 1 M to obtain an average distance of 6.5 Å.

9.2.3. Photoinduced Electron Transfer

The third mechanism for quenching is photoinduced electron transfer (PET). In PET a complex is formed between the electron donor D_P and the electron acceptor A_P, yielding $D_P{}^+A_P{}^-$ (Figure 9.9). The subscript P is used to identify the quenching as due to a PET mechanism. This charge transfer complex can return to the ground state without emission of a photon, but in some cases exciplex emission is

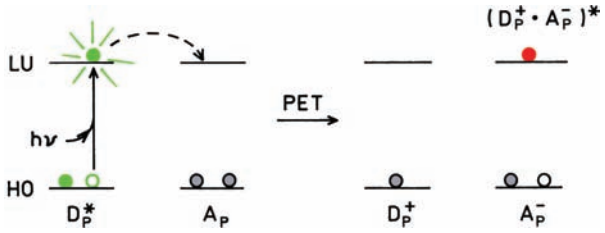

Figure 9.9. Molecular orbital schematic for photoinduced electron transfer.

observed. Finally, the extra electron on the acceptor is returned to the electron donor.

The terminology for PET can be confusing because the excited fluorophore can be either the electron donor or acceptor. The direction of electron transfer in the excited state is determined by the oxidation and reduction potential of the ground and excited states. When discussing PET the term donor refers to the species that donates an electron to an acceptor. In PET the terms donor and acceptor do not identify which species is initially in the excited state. This is different from RET, where a fluorophore is always the donor.

The nature of PET quenching is clarified by examining several examples. The more common situation is when the excited state of a fluorophore acts as an electron acceptor (Table 9.1). One typical example is an electron-rich species such as dimethylaniline (DMA), which can donate electrons to a wide range of polynuclear aromatic hydrocarbons, which act as electron acceptors. Electron transfer is even more favorable to electron-deficient species like cyanonaphthalenes. There are some unusual PET pairs, such as indole donating to pyrene and dienes donating to cyanoanthracene. This table is not exhaustive, but provides only examples of PET pairs.

Table 9.1. PET Quenching Where the Fluorophore Is the Electron Acceptor

$F^* - Q \rightarrow (F^- \cdot Q^+)^* \rightarrow$ heat or exciplex	
Fluorophore (PET acceptor)	Quencher (PET donor)
Polynuclear aromatic hydrocarbons	Amines, dimethylaniline
2-Cyanonaphthalenes	Dimethylaniline
7-Methoxycoumarin	Guanine monophosphate
Pyrene	Indole
9-Cyanoanthracene	Methyl indoles
9,10-Dicyanoanthracene	Dienes and alkenes, alkyl benzenes
Anthraquinones	Amines
Oxazine	Amines

These quenching reactions are described in [38–48].

Table 9.2. PET Quenching Where the Fluorophore Is the Electron Donor

$F^* - Q \rightarrow (F^+ \cdot Q^-)^* \rightarrow$ heat or exciplex	
Fluorophore (PET donor)	Quencher (PET acceptor)
Indole or NATA	Imidazole, protonated
Indole	RCO_2H, but not RCO_2^-
Tryptophan	Acrylamide, pyridinium
Carbazole	Halocarbons; trichloroacetic acid
Indole	Halocarbons
$[Ru(bpy)_3]^{2+}$	Methylviologen
Dimethoxynaphthalene	N-methylpyridinium

These quenching reactions are described in [49–57].

PET quenching can also occur by electron transfer from the excited fluorophore to the quencher (Table 9.2). Examples include electron transfer from excited indoles to electron-deficient imidazolium or acrylamide quenchers. Quenching by halocarbons can also occur by electron transfer from the fluorophore to the electronegative halocarbon. Electron-rich dimethoxynaphthalene can donate electrons to pyridinium. And finally there is the well-known example of electron transfer from excited $[Ru(bpy)_3]^{2+}$ to methylviologen.

9.3. ENERGETICS OF PHOTOINDUCED ELECTRON TRANSFER

Photoinduced electron transfer has been extensively studied to understand quenching and to develop photovoltaic devices. For quenching by intersystem crossing and electron exchange it is difficult to predict the efficiency of quenching. Hence the description of these quenching processes is mostly based on experience rather than calculation. In contrast PET is more predictable because the possibility of electron transfer can be predicted from the redox potentials of the fluorophore and quencher.

Most descriptions of PET derive the energy change due to electron transfer starting with the basic principles of electrochemistry. This can be confusing because of the sign conventions used in redox chemistry. Hence we will start with the final result and then explain its origin. Figure 9.10 shows an energy diagram for PET with the excited molecule being the electron donor. For clarity, this diagram does not include diffusion that may be needed to bring D_P and A_P into contact. We are assuming the molecules are already in contact. Upon excitation the electron donor transfers an

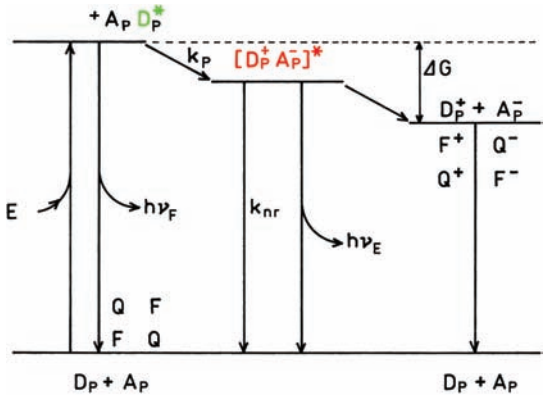

Figure 9.10. Energy diagram for photoinduced electron transfer. The excited molecule is assumed to be the electron donor. ν_F and ν_E are emission from the fluorophore and exciplex, respectively.

electron to the acceptor with a rate $k_P(r)$, forming the charge-transfer complex $[D_P^+ A_P^-]^*$. This complex may emit as an exciplex or be quenched and return to the ground state.

The important part of this process is the decrease in total energy of the charge transfer complex. The energy decreases because the ability to donate or accept electrons changes when a fluorophore is in the excited state. Excitation provides the energy to drive charge separation. D_P and A_P do not form a complex when both are in the ground state because this is energetically unfavorable. The energy released by electron transfer can also change if the ions become solvated and/or separated in a solvent with a high dielectric constant.

The energy change for PET is given by the Rehm-Weller equation:

$$\Delta G = E(D^+/D) - E(A/A^-) - \Delta G_{00} - \frac{e^2}{\varepsilon d} \quad (9.7)$$

In this equation the reduction potential $E(D^+/D)$ describes the process

$$D_P^+ + e \rightarrow D \quad (9.8)$$

and the reduction potential $E(A/A^-)$ describes the process

$$A_P + e \rightarrow A_P^- \quad (9.9)$$

ΔG_{00} is the energy of the $S_0 \rightarrow S_1$ transition of the fluorophore, which can be either D_P or A_P. The last term on the right is the coulombic attraction energy experienced by the ion pair following the electron transfer reaction; ε is the dielectric constant of the solvent, and d is the distance between the charges.

The Rehm-Weller equation has its origin in the free energy change for moving charge in an electric potential. The energy released by a mole of electrons moving in a potential ΔE is given by

$$\Delta G = -nF\Delta E \quad (9.10)$$

where n is the number of electrons in the reaction, ΔE is the potential, and F is the Faraday constant, which is the charge on 1 mole of electrons. From this expression one can see that ΔE is positive for a thermodynamically favored reaction. This convention is confusing because we normally associate a negative value with a favored reaction.

In describing the PET process we need to consider the redox potential of D_P and A_P and the energy of the incident light. Hence it is important to know the conversion factors. For a mole of electrons moving across a potential difference of ΔE = 1 V the energy is 1 eV = 23.06 kcal, so that

$$\Delta G \text{ (in kcal/mol)} = -23.06n\Delta E \quad (9.11)$$

We also need to convert a mole of absorbed photons into kcal/mole. The energy in a mole of photons is given by

$$\Delta E \text{ (kcal/mol)} = 28{,}600/\lambda \text{ (nm)} \quad (9.12)$$

A mole of 400-nm photons equals 71.5 kcal, and a mole of 600 nm photons equals 47.7 kcal.

Studies of PET are usually performed in polar solvents, frequently acetonitrile, which is a common solvent used when determining the reduction potentials. For complete separation of one electron charge in acetonitrile $e^2/\varepsilon d$ is equal to 1.3 kcal/mole = 0.06 eV. This term usually makes a small contribution to the overall energy change for PET.

The form of eq. 9.7 can now be understood intuitively. The terms ΔG_{00} and $e^2/\delta d$ appear with a negative sign because the energy will be lost when the light energy is dissipated and the ions experience coulombic attraction. $E(D^+/D)$ and $E(A/A^-)$ appear with opposite signs because these are both reduction potentials. However, D is oxidized to D^+ and A is reduced to A^-. For the same reaction the oxidation potential is the negative of the reduction potential.

Why is the energy of the charge-transfer state lower than the energy before electron transfer? This can be under-

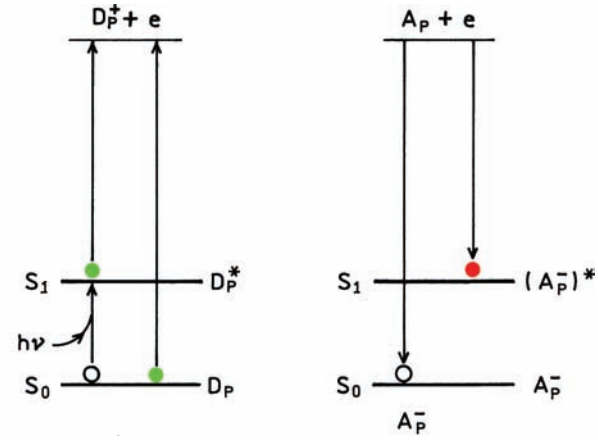

Figure 9.11. Changes in electron affinity between the S0 and S1 states.

stood by considering the energy required to remove an electron completely from the electron donor (Figure 9.11), which is the energy needed to ionize a donor fluorophore. When the fluorophore is in the excited state the electron is at a higher energy level than a ground-state electron. Hence it will require less energy to remove an electron from the S_1 (LU) state then from the S_0 (HO) state. This means the donor fluorophore in the S_1 state has a higher propensity to donating an electron.

Now consider a quencher that is an electron acceptor (Figure 9.11). The energy released on binding the electron is larger if the electron returns to the S_0 state than to the S_1 state. The electron can return to the lowest orbital of the quencher because the donor–acceptor complex is momentarily an excited-state complex. When the electron acceptor is in the excited state there is a place for the electron to bind to the lowest orbital.

9.3.1. Examples of PET Quenching

The energetics of PET quenching is clarified by specific examples. Figure 9.12 shows lifetime Stern-Volmer plots for quenching of three coumarin derivatives by ethylaniline (EAN).[58] All three coumarins have a trifluoromethyl group, which increases their ability to accept electrons from EAN. Based on the chemical structures we expect EAN to be the electron donor and the coumarins to be the electron acceptors. The largest Stern-Volmer constant is for the amino derivative C151, with lesser amounts of quenching for the methylated C522 and C152. The methylated coumarins are less quenched than the amino coumarin, which is consistent with the well-known electron-donating properties of methyl

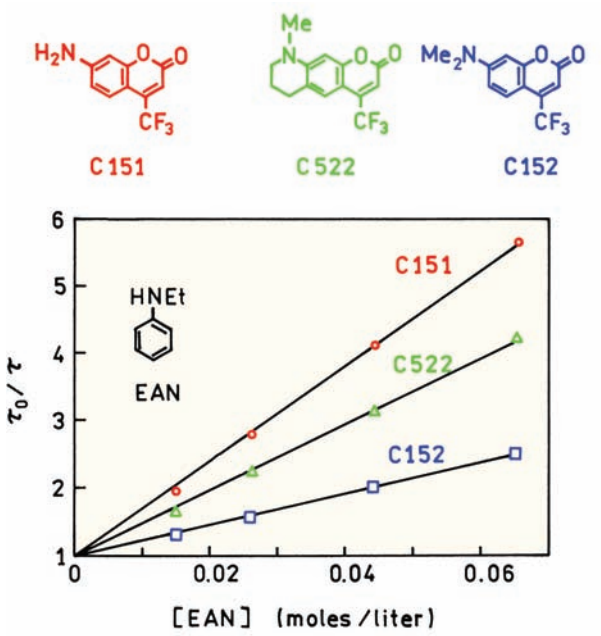

Figure 9.12. Quenching of coumarin derivatives by ethylaniline. Revised and reprinted with permission from [58]. Copyright © 2000, American Chemical Society.

groups. The additional methyl groups decrease the ability of the coumarin to accept electrons.

Figure 9.13 shows a similar PET quenching experiment, but one using a single fluorophore, Neutral Red (NR), and three different aromatic amine quenchers.[58–59] The

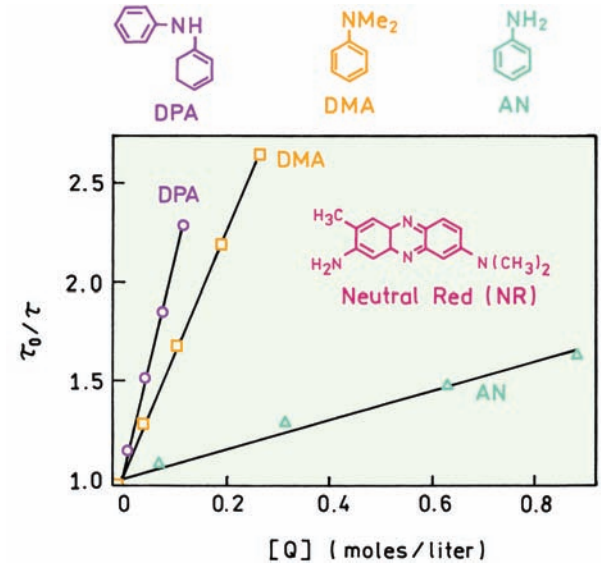

Figure 9.13. PET quenching of Neutral Red by aromatic amines. Revised from [59].

Table 9.3. Reduction Potentials and Quenching Constants for PET Quenching

Acceptor fluorophore	Donor quencher	E_{00} (eV)	$E(A/A^-)$ (volts)	$E(D^+/D)$ (volts)	ΔG (eV)	ΔG (kcal/mole)	τ_0 (ns)	k_q (M^{-1} s^{-1})
C151	EAN	2.98	–1.565	0.80	–0.67	–15.45	5.18	10.9 x 10^9
C522	EAN	2.70	–1.653	0.80	–0.31	–7.15	5.48	5.3 x 10^9
C152	EAN	2.76	–1.626	0.80	–0.39	–8.99	1.96	9.1 x 10^9
Neutral Red	DPA	2.41	–1.51	0.64	–0.32	–7.38	4.15	3.55 x 10^9
Neutral Red	DMA	2.41	–1.51	0.76	–0.20	–4.61	4.15	1.49 x 10^9
Neutral Red	AN	2.41	–1.51	0.93	–0.03	–0.69	4.15	0.24 x 10^9

ΔG (eV) = $E(D^+/D) - E(A/A^-) - E_{00} - 0.06$.
Data from [58–59].

amount of quenching increases when the quenchers have methyl or phenyl groups on the amino group, which increased the electron density and propensity of the quenchers to donate electrons.

It is instructive to examine calculations of the ΔG values for PET (Table 9.3). The E_{00} values were obtained from the intersection of the normalized absorption and emission spectra of the fluorophores, and converted to eV using eqs. 9.11 and 9.12. These values, and the polarographic reduction potentials, can be used with eq. 9.7 to calculate which coumarin has a higher propensity to undergo PET. The ΔG values for electron transfer for all three coumarins are negative, showing that PET is energetically possible. The larger value of E_{00} for C151 results in the largest value of ΔG and the largest amount of PET quenching. Table 9.3 also contains Rehm-Weller calculation for quenching of NR.

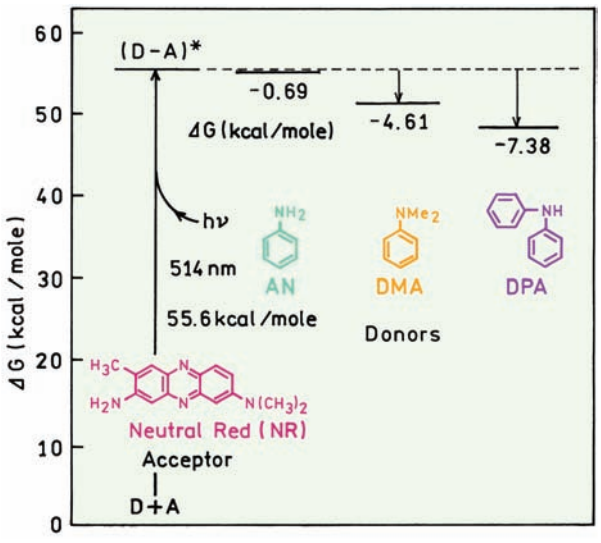

Figure 9.14. Energy diagram for quenching of Neutral Red with aromatic amines. Data from [59].

The PET reaction releases more energy when the aniline contains the additional electron-donating groups. The largest bimolecular quenching constant was found for the PET reaction with the most negative ΔG value. There is a strong correlation of larger bimolecular quenching constants with more negative ΔG values.

Figure 9.14 shows a schematic of the energy changes upon PET to NR. Excitation at 514 nm adds 55.6 kcal/mole to NR. The amines that have the largest bimolecular constants also show the largest decrease in energy when the charge transfer complex is formed. Examination of this figure and Table 9.3 reveals why it is intuitively difficult to look at the reduction potential of D_P and A_P to predict the energy change for the reaction. The overall ΔG is the difference of three large numbers that all contribute to ΔG for the reaction.

Examination of the k_q values in Table 9.3 shows a strong dependence on ΔG for quenching of NR, but a weaker dependence on ΔG for quenching of the coumarins. It is easy to understand why the correlation is variable. Figure 9.15 shows k_q values for amine quenching of Neutral Red. From left to right the reduction potential $E(D^+/D)$ of the amine increases. Using eq. 9.7 shows that ΔG for the reaction is less negative for AN than for the other quenchers. This indicates that AN binds its electrons more tightly than the other two amines in Figure 9.15, which in turn results in less efficient PET and less efficient quenching. However, if ΔG is more negative than –0.5 eV, then PET formation and quenching is 100% efficient, so that small changes in ΔG. do not affect the efficiency. In Table 9.3 the ΔG values for quenching of the coumarins were –0.31 eV, or more negative, so that all three coumarins were efficiently quenched.

The rate of PET can be measured using time-resolved measurements. However, if quenching is almost 100% efficient then the unusual quenching experiment reveals the value of k_q. The rate of PET will not have a large effect on

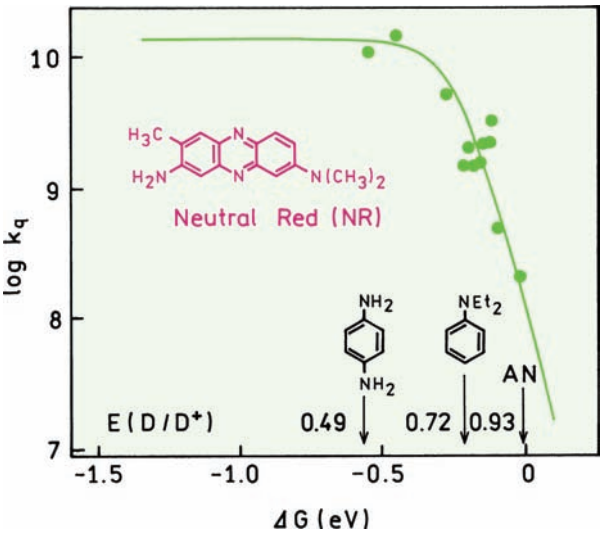

Figure 9.15. Correlation of k_q for PET quenching of Neutral Red with ΔG for the reaction. Revised from [59].

k_q because $k_p(r)$ is much larger than k_q and PET is limited by the rates of diffusion. In order to study the electron-transfer rate it is necessary to eliminate the effect of diffusion. However, high quencher concentrations are required to obtain contact quenching without diffusion. The intensity decays of the three coumarin derivatives were examined in neat DMA (Figure 9.16).[60] In pure DMA the fluorophores are surrounded by electron donors so no diffusion is needed to bring D_P and A_P into contact. Hence the intensity decays should reflect the electron-transfer rate $k_p(r)$ rather than the diffusion-controlled collision rate. The most rapid intensity decay was observed for C151 where ΔG = –15.5 kcal/mole. Slightly slower decays were observed for C152 and C522, where ΔG is less negative.

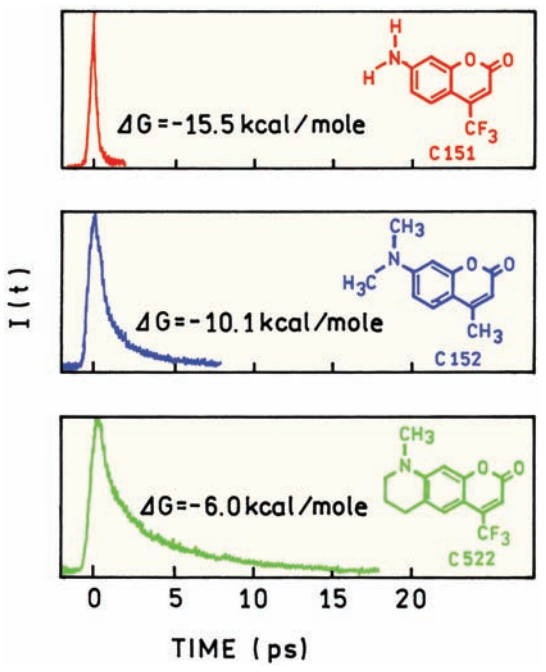

Figure 9.16. Time-dependent decays of coumarin derivatives in neat DMA. Revised and reprinted with permission from [60]. Copyright © 1993, American Chemical Society.

9.3.2. PET in Linked Donor–Acceptor Pairs

The need for high quencher concentrations can be avoided using covalently linked D–A pairs. One example is shown in Figure 9.17, where the electron acceptor methylviologen (MV^{2+}) is covalently linked to 1,8-naphthalimide. The spacer contained n = 2 to 6 methylene groups.[61] In this case the naphthalimide fluorophore is the electron donor and MV^{2+}

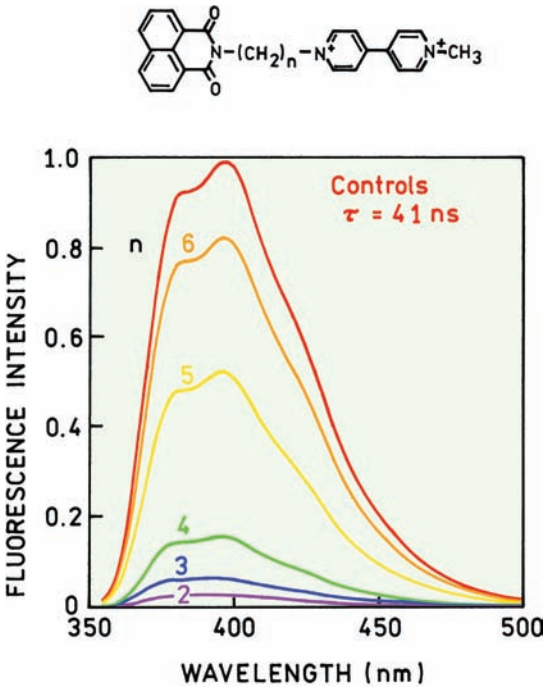

Figure 9.17. Emission spectra of covalently linked 1,8-naphthalimide and methylviologen. n is the number of methylene groups. The control compound lacked the methylviologen acceptor, and instead had a linked pyridine group with the same number of methylene groups. Revised and reprinted with permission from [61]. Copyright © 2000, American Chemical Society.

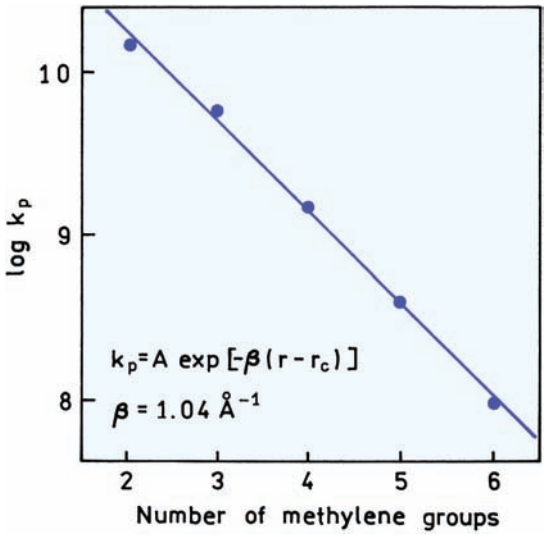

Figure 9.18. Distance dependence of the electron-transfer rate from 1,8-naphthalimide to covalently linked methylviologen. β = 1.32 per methylene group (assuming 1.27 Å per methylene group). Revised and reprinted with permission from [61]. Copyright © 2000, American Chemical Society.

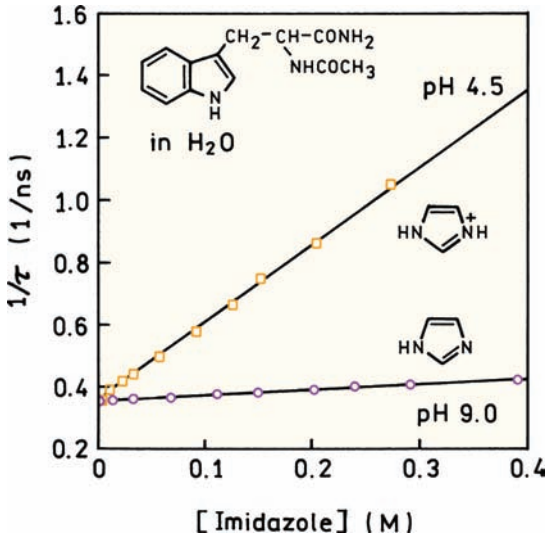

Figure 9.19. Quenching of NATA by imidazole (pH 9) and imidazolium (pH 4.5). Revised from [62].

the electron acceptor. The intensity decreases as the number of methylene groups decreases. The D–A pair was examined in dilute aqueous solution. In highly dilute solution, collisions between D and A groups on different molecules is not significant. Hence the change in donor intensity reflects the effect of distance on the rate of electron transfer. There may also be a component due to flexing of the D–A pair during the excited-state lifetime.

The intensity data were used to calculate the rates of energy transfer. This was accomplished by using eq. 9.4, where Q is the relative intensity and $\gamma = 41$ ns^{-1} (Figure 9.18). The rate of electron transfer decreases by a factor of 180 as n increases from 2 to 6, which is an increase in distance of about 5 Å. This result shows the dramatic decrease in $k_p(r)$ with distance.

9.4. PET QUENCHING IN BIOMOLECULES

9.4.1. Quenching of Indole by Imidazolium

Intrinsic fluorescence from tryptophan residues is frequently used to study the properties of proteins. In order to interpret the tryptophan emission it is important to understand the effects of nearby amino acid side chains. The amino acid histidine has an imidazole group in its side chain. Since the pK_a of this group is near 6.5, it can be protonated or unprotonated depending on the pH and the charges on other nearby amino-acid side chains. Proteins frequently display pH-dependent changes in intensity near pH 7, suggesting an effect due to the imidazole–imidazolium equilibrium.

Figure 9.19 shows the inverse lifetime of NATA in an aqueous solution that contains imidazole.[62] At pH 4.5 there is strong quenching of NATA. At pH 9, at the same imidazole concentrations, there is little quenching. Since NATA is uncharged this difference is not due to electrostatic interactions. The indole ring in the excited state donates an electron to the imidazolium because PET is energetically favorable to this electron-deficient species. Uncharged imidazole does not accept the electron, so quenching does not occur at pH 9.

9.4.2. Quenching by DNA Bases and Nucleotides

Fluorescently labeled oligomers are widely used in DNA analysis and biotechnology. Hence there is interest in understanding what factors influence the intensity of covalently bound fluorophores. The extent of quenching depends on the base and the structure of the fluorophore.[43,63] Among the bases guanine appears to be the most efficient quencher, probably because it has the highest tendency to donate an electron. Figure 9.20 shows the lifetime distributions for oligomers labeled with MR121.[64] If the oligomer does not contain guanine, the decay of MR121 is a single exponential with $\tau = 2.72$ ns. The presence of a single guanine as the second base results in a short-lived component with $\tau = 0.43$ ns that is due to PET quenching.

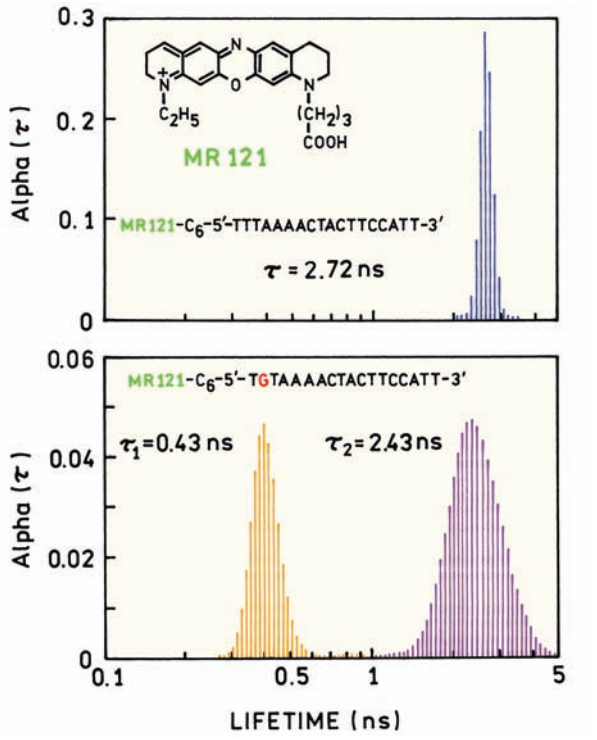

Figure 9.20. Lifetime distribution of MR121-labeled oligomers with T or G as the second base. Revised from [64].

One can expect the quantum yields and lifetimes of labeled oligomers to depend on the base sequence near the fluorophore.

PET has been used to study electron transfer along double-helical DNA.[65] Figure 9.21 shows a DNA hairpin that contains a covalently bound stilbene residue at the bending site. A single guanine residue was positioned next to the stilbene or spaced by several base pairs. The lifetimes decrease dramatically as the guanine approaches the stilbene residue with $\beta = 0.64$ Å^{-1}. One can imagine PET quenching being used to develop molecular beacons or DNA hybridization assays based on quenching by guanine residues.

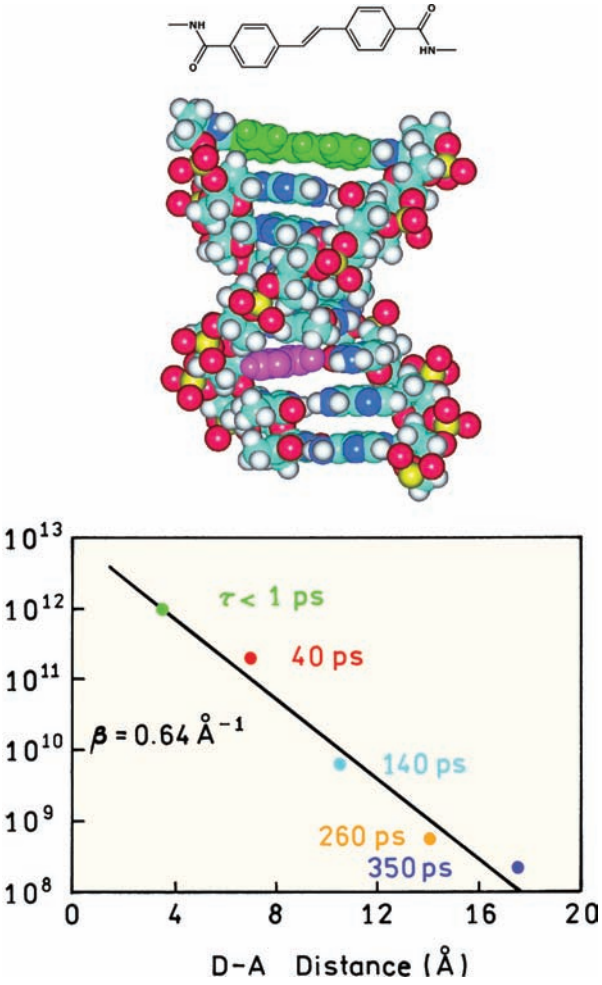

Figure 9.21. PET quenching of oligomers labeled with stilbene (green) and containing a single guanine residue (red base). From left to right in the lower panel this guanine is the 1st, 2nd, 3rd, 4th, or 5th base pair away from the stilbene. Revised from [65].

9.5. SINGLE-MOLECULE PET

During the past 10 years fluorescence technology has advanced to allow studies of single molecules. This is usually accomplished using fluorophores immobilized on a surface and confocal optics to reject out-of-focus light. Single-molecule detection (SMD) has been extended to PET quenching.[66–67] Figure 9.22 shows the intensity versus time observed for single fluorophores on a glass surface dissolved in a thin layer of a viscous polymer. The fluorophores are dimers of perylene connected directly or by three phenyl groups. The phenyl groups are thought to act as a nonconducting bridge. The intensities were found to blink on and off. Under the same experimental conditions the monomer control compound did not show blinking. The on and off blinking of these perylene dimers was assigned to fluctuations in the conformations of the molecule between one favorable for PET, when the molecules are dark, or a conformation unfavorable for PET, where the molecules are fluorescent. Single fluorophores of many types are known to display blinking due to transitions to the triplet state (Chapter 23). In Figure 9.22 the off times were claimed to be too long to be due to triplets, even in a rigid

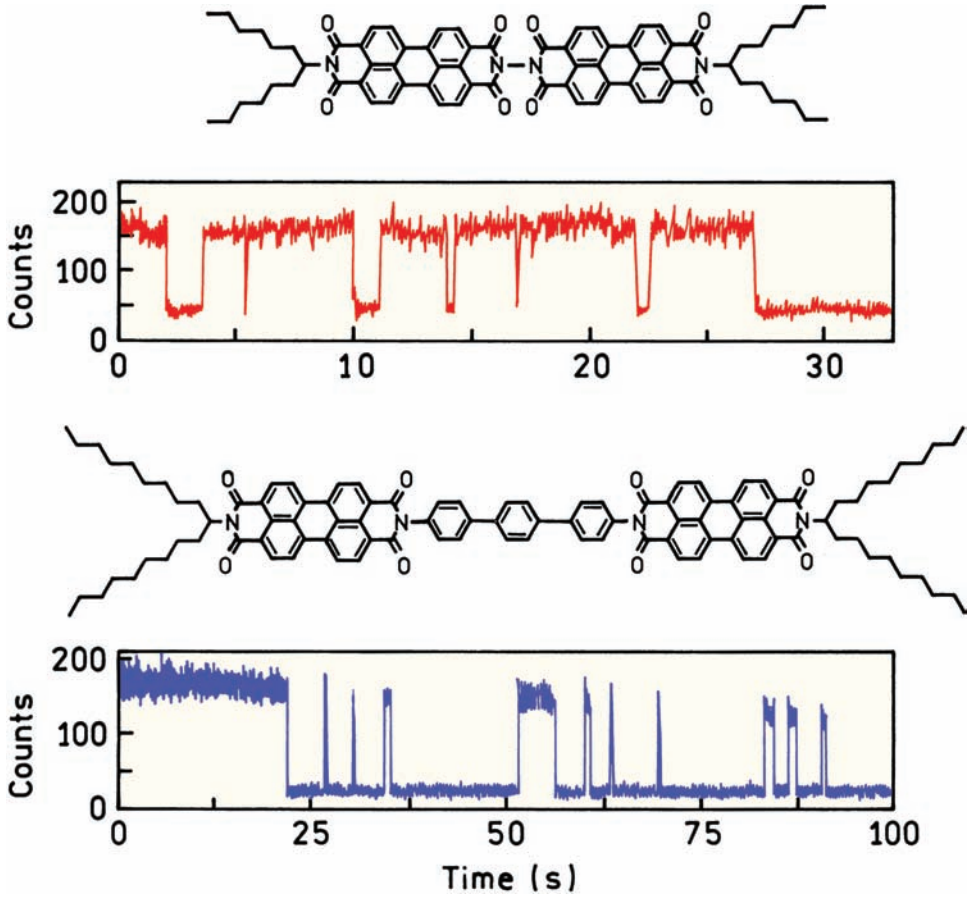

Figure 9.22. Single-molecule intensity traces for two bis-perylene compounds. The intensity axis is photons per 20 ms. Revised and reprinted with permission from [67]. Copyright © 2003, American Chemical Society.

polymer, so the blinking was assigned to conformational fluctuations which affected the rate of PET.

9.6. TRANSIENT EFFECTS IN QUENCHING

We have now seen that collisional quenching occurs by several mechanisms. All these mechanisms have the same requirement for molecular contact between the fluorophore and quencher. As a result quenching requires diffusion to bring the molecules into contact. Without diffusion high concentrations of quencher near 1 M are necessary to statistically position a quencher adjacent to the fluorophore at the moment of excitation.

For diffusive or collisional quenching, we stated in Chapter 8 that the lifetime decreases in proportion to the decrease in fluorescence intensity. If the decay was a single exponential before quenching, we assumed the decay remained a single exponential in the presence of quencher. In reality, intensity decays become non-exponential in the presence of collisional quenching. By non-exponential we mean not described by a sum of exponentials. This effect is due to the so-called transient effects in quenching.[68] For small amounts of quenching in fluid solvents, these effects are barely noticeable. For larger amounts of quenching, especially in moderately viscous solvents, the intensity decays become strongly non-exponential.

The theory for transient effects is complex and has been presented in a monograph on diffusion-controlled reactions.[69] This effect was first identified by Smoluchowski, who considered diffusion-controlled reactions between particles in solution.[70] The rate constant for reaction between the particles was shown to be time-dependent

$$k(t) = 4\pi RN'D\left[1 + R(\pi Dt)^{-1/2}\right] \qquad (9.13)$$

where R is the interaction radii (sum of the radius of the fluorophore (F) and quencher (Q)), $N' = 6.02 \times 10^{20}$, and D is

the sum of the F and Q diffusion coefficients. The time dependence originates with the random distribution of fluorophores and quenchers at the moment of excitation. Some fluorophore–quencher pairs will be in close proximity, and others will be more widely spaced. The fluorophores with a closely located quencher are extinguished rapidly. With time following excitation, the ensemble of fluorophores evolves, and the fluorophores that remain in the excited state longest are those that were most distant from the closest quencher at the moment of excitation. The time-dependent rate constant decreases from an initially high value to the diffusion limited value ($k_q = 4\pi RN'D$). The intensity decay in the presence of collisional quenching can be obtained by integration of the differential equation describing $dI(t)/dt$ that includes the time-dependent rate constant. This yields

$$I(t) = I_0 \exp(-t/\tau - 2bt^{1/2}) \tag{9.14}$$

where τ is given by

$$\frac{1}{\tau} = \frac{1}{\tau_0} + k_q[Q] \tag{9.15}$$

and

$$b = 4R^2N'(\pi D)^{1/2}[Q] \tag{9.16}$$

While these equations seem complex, the actual situation is still more complex. The Smoluchowski model assumes that the fluorophore is instantaneously deactivated upon contact with the quencher, which results in an infinite quencher concentration gradient around the fluorophore. Also, the Smoluchowski model assumes no quenching in the absence of molecular contact. These assumptions have been modified to allow more realistic modeling of the quenching process.[71–72] These quenching models are shown schematically in Figure 9.23. The radiation boundary condition (RBC) model assumes that quenching occurs with a finite rate constant k when F and Q are in contact (Figure 9.23). For the Smoluchowski model $k(r) = 4$ when F and Q are in contact, and $k(r) = 0$ otherwise.

Another model for quenching assumes that the quenching rate is dependent on the F-Q distance. In this model the quenching constant is assumed to depend on the distance between the fluorophore and quencher. In the previous sections we saw that the rates of electron exchange and electron transfer depend exponentially on distance. A similar

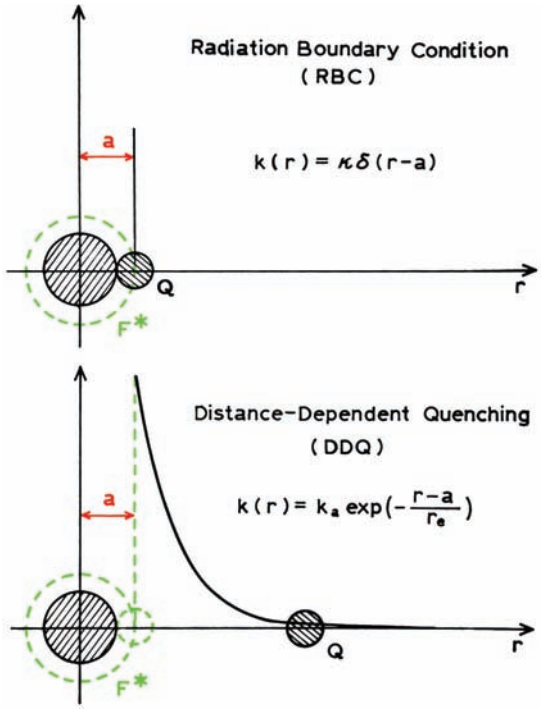

Figure 9.23. Comparison of the RBC and DDQ models for collisional quenching of fluorescence. Revised and reprinted with permission from [80]. Copyright © 1996, American Chemical Society.

dependence on distance has been reported for intersystem crossing.[8] This effect can be accounted for using the distance-dependent quenching (DDQ) model. For this model of distance-dependent interactions the rate of quenching at an F–Q distance r is given by

$$k(r) = k_a \exp\left(-\frac{r-a}{r_e}\right) \tag{9.17}$$

where r_e is the characteristic distance, and k_a is the rate of reaction at the distance of closest approach (a), typically 5–7 Å. This expression has the same form as eq. 9.2. The time-dependent rate constant is given by

$$k(t) = \frac{4\pi}{C_q^0}\int_a^\infty r^2 k(r) C_q(r,t)\, dr \tag{9.18}$$

where $C_q(r,t)$ is the concentration of the quencher molecules at distance r from the excited fluorophore at time instant t and C_q^0 is the bulk quencher concentration. This expression says that the bimolecular quenching constant at any time is given by the values of $k(r)$ averaged over the

concentration gradient around the fluorophore at some instant in time. The use of these quenching models requires rather complex theory and analysis. For the Smoluchowski, RBC, or DDQ models the intensity decay is given by

$$I(t) = I_0 \exp(-t/\tau_0) \exp\left[-[Q]\int_0^t k(t)\,dt\right] \qquad (9.19)$$

where $k(t)$ is the time-dependent rate constant. For the RBC model $k(t)$ is given by[73–76]

$$k(t) = \frac{4\pi RDN}{1 + (D/\kappa R)}\left[1 + \frac{\kappa R}{D}\exp(X^2)\,erfc(X)\right] \qquad (9.20)$$

$$X = \frac{(Dt)^{1/2}}{R}\left[1 + \frac{\kappa R}{D}\right] \qquad (9.21)$$

The function $erfc(X)$ is the complement of the error function:

$$erfc(X) = \frac{2}{\pi^{1/2}}\int_X^\infty \exp(-z^2)\,dz \qquad (9.22)$$

For the DDQ model analytical expressions for $k(t)$ are not yet known, so numerical procedures are often used to calculate intensity decay $I(t)$.[77–83] Several reports have focused on the analysis of decays with transient effects.[84–87]

It is useful to visualize how the quenching constant depends on time. The values of $k(t)$ are shown in Figure 9.24 for the Smoluchowski model and for the RBC model with various values of 6. For a diffusion coefficient near 10^{-6} cm^2/s the transient effects are mostly complete in 10 ps, and are no longer present at 1 ns. For times over 1 ns the value of $k(t)$ becomes equal to the usual bimolecular quenching constant (eq. 8.11). At short times the values of $k(t)$ are initially larger than the calculated value of k_q. This effect is due to the rapid quenching of closely spaced F–Q pairs. In the Smoluchowski model the value of $k(t)$ diverges to infinity at short times. This difficulty is avoided in the RBC model, where the maximal rate is limited by the value of κ. As κ increases, the RBC model becomes identical with the Smoluchowski model.

Equation 9.18 indicates that the concentration of quencher $C_q(r,t)$ around the fluorophore changes with time and distance. This seems counterintuitive because the fluorophore is in equilibrium with the bulk concentration of quencher. This effect can be understood by considering the population of fluorophores being observed (Figure 9.25). The surfaces show the concentration of quencher around the fluorophore following pulsed excitation.[83] At $t = 0$ there is a uniform quencher concentration around the fluorophore. As time increases the quencher concentration around the fluorophore decreases at short distances, with the effect being larger for the DDQ model than for the RBC model. Since the fluorophore and quencher are not destroyed upon quenching, it is not immediately obvious why $C_q(r,t)$ changes.

In order to understand the changes in $C_q(r,t)$ we need to recall that we are observing an ensemble of fluorophores. At short times following excitation there is rapid quenching of the closely spaced F–Q pairs, mostly without the need for diffusion. These pairs are quenched with the larger rate constant $k(r)$. At longer times all the closely spaced pairs have

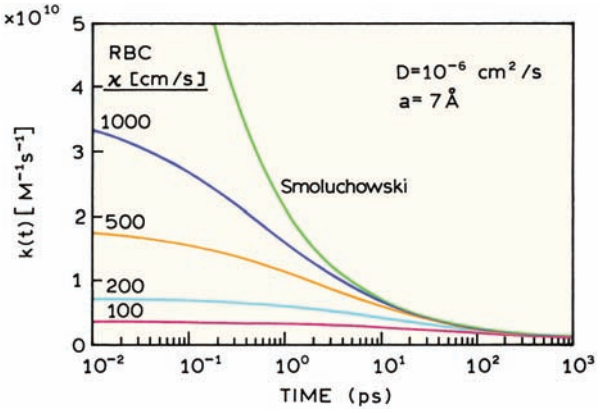

Figure 9.24. Time-dependent rate constants for the Smoluchowski and RBC models. From [88].

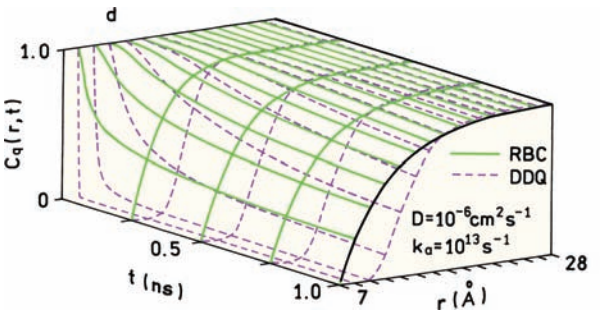

Figure 9.25. Simulations of the quencher concentration $C_q(r,t)$ around the fluorophores for various times and distances. The solid and dashed lines are for the RBC and DDQ models, respectively. Reprinted from [83].

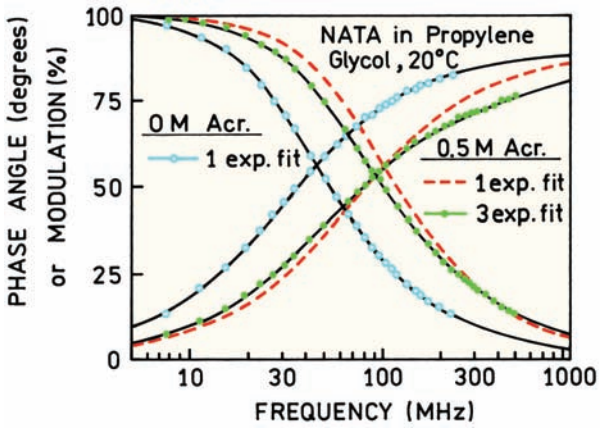

Figure 9.26. Frequency-domain intensity decays of NATA in propylene glycol in the absence and presence of 0.5 M acrylamide. Revised from [89].

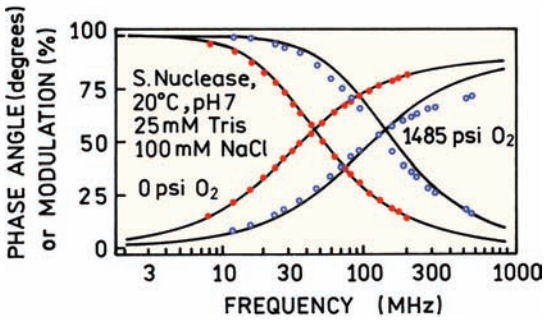

Figure 9.27. Frequency response of staphylococcal nuclease in the absence (●) and presence (○) of 0.144 M oxygen. The solid lines show the best single exponential fits to the data. The values of P for the single exponential fits at 0 and 1485 psi O_2 are 5.9 and 265, respectively. From [90].

decayed, and the rate of quenching becomes limited by diffusion with a bimolecular rate constant k_q.

As time proceeds the observed fluorophore population is changing from closely spaced to more distant F–Q pairs. The quencher concentration around the ground-state fluorophores is not changing. The excited fluorophore population is changing, so that the fluorophores remaining in the excited state were located further from a quencher at the moment of excitation.

9.6.1. Experimental Studies of Transient Effects

Figure 9.26 shows frequency-domain intensity decays for NATA in propylene glycol.[89] In the absence of quenching, the frequency-domain intensity decay reveals a single exponential decay. In the presence of 0.5 M acrylamide the decay becomes strongly heterogeneous, and cannot be fit by a single exponential decay law, $\chi_R^2 = 240$, but could be fit using a triple exponential decay. Transient effects can also be observed for proteins.[90–91] The single-tryptophan protein staphylococcal nuclease is known to display a dominant single exponential decay, as seen by the overlap with the single decay time model (Figure 9.27). When quenched by oxygen the intensity decay is no longer a single exponential. Oxygen diffusion is rapid, which minimizes the transient part of the rate constant (eq. 9.13). Larger effects can be expected if diffusion is slower or if the solution is somewhat viscous. These transient terms can be accounted for using the multi-exponential model. However, the decay components do not directly represent any molecular property of the sample.

The complex intensity decays observed in the presence of quenching can be explained by the transient models.[92–93] This is illustrated in Figure 9.28 for quenching of NATA by acrylamide.[78] The frequency-domain data could not be explained by the RBC model, but were consistent with the DDQ model. This indicates that the quenching rate displays

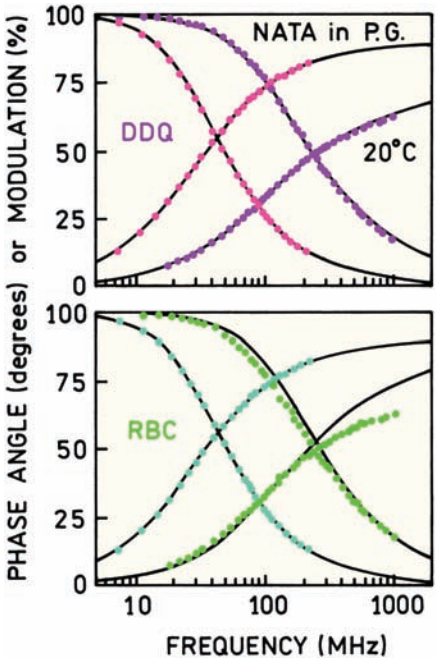

Figure 9.28. Frequency-domain intensity decays of NATA in propylene glycol at 20°C in the presence of increasing (left to right) concentrations of acrylamide (1.5 M). The solid lines (top) show the best fit to the DDQ model using a = 5 Å and r_c = 0.319 Å. The solid lines (bottom) show the best fit to the RBC model using a = 5 Å. Revised with permission from [78]. Copyright © 1994, American Society for Photobiology.

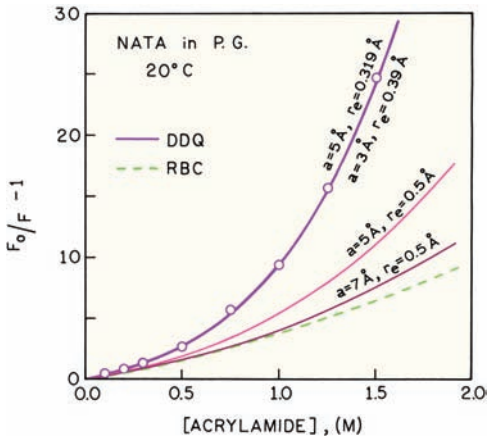

Figure 9.29. Stern-Volmer plots for NATA in propylene glycol at 20°C quenched by acrylamide (○). The solid lines represent the calculated values of $(F_0/F - 1)$ using the parameter values from the DDQ model for a = 7 Å and r_c = 0.5 Å, a = 5 Å and r_c = 0.5 Å, and a = 5 Å and r_c = 0.319 Å. The dashed line represents the RBC model using a = 5 Å. Reprinted with permission from [78]. Copyright © 1994, American Society for Photobiology.

an exponential dependence on distance, and that quenching is not an all-or-none process that occurs only at the contact distance.

An important result from the transient analysis is an explanation for the upward curvature seen in many Stern-Volmer plots.[78–79] The acrylamide Stern-Volmer plot for NATA shows substantial upward curvature in the moderately viscous solvent propylene glycol (Figure 9.29). While the curvature could be explained by a weak static quenching constant, or by a sphere of action, the upward curvature is a natural consequence of distance dependent quenching. This explanation of upward deviations in the Stern-Volmer plots is more satisfying because there is a single molecular interaction, the exponential distance dependence of quenching, which explains the time-dependent and steady-state data.

The transient model can also explain upward-curving Stern-Volmer plots in proteins. This is illustrated by the quenching of staphylococcal nuclease by acrylamide[91] (Figure 9.30). In this case the calculated curve for the intensity data was obtained using the Smoluchowski model (eq. 9.14). This equation can be integrated to obtain the Stern-Volmer equation with transient effects:[68]

$$\frac{F_0}{F} = \frac{1 + K_D[Q]}{Y} \qquad (9.23)$$

where $K_D = k_q \tau_D$ and

$$Y = 1 - \frac{b\sqrt{\pi}}{a} \exp(b^2/a)\, erfc(b/\sqrt{a}) \qquad (9.24)$$

$$a = \frac{1}{\tau_0} + k_q[Q] \qquad (9.25)$$

with b as defined in eq. 9.16.

The validity of distance-dependent quenching is supported by an observation that cannot be explained by other models. In frozen solution, where diffusion does not occur, one still observes quenching of NATA by acrylamide (Figure 9.31). The magnitude of the effect cannot be explained

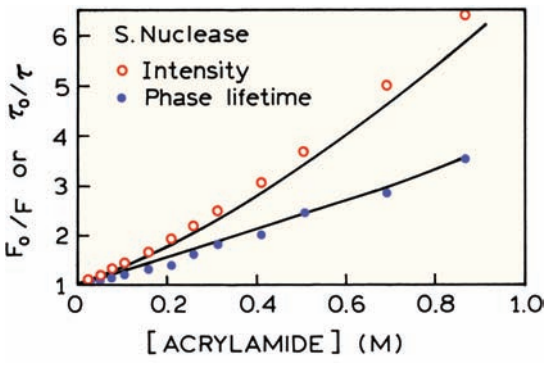

Figure 9.30. Intensity and phase-lifetime Stern-Volmer plots for the acrylamide quenching of staphylococcal nuclease A at 20°C, pH 7. Lifetimes were measured at 50 MHz. Solid lines are a simultaneous fit with R (fixed) = 7 Å, τ_0 = 4.60 ns, and D = 0.058 x 10^{-5} cm^2/s. Revised from [91].

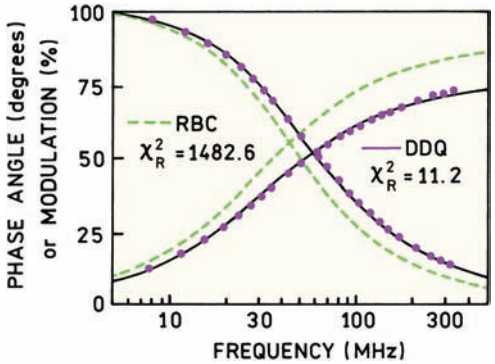

Figure 9.31. Frequency-response of the NATA intensity decay in propylene glycol at –60°C. The data (●) are for NATA with 1.048 M acrylamide at –60°C, and the solid line represents the best DDQ fit. The dashed line shows the RBC fit with D = 0. Reprinted with permission from [78]. Copyright © 1994, American Society for Photobiology.

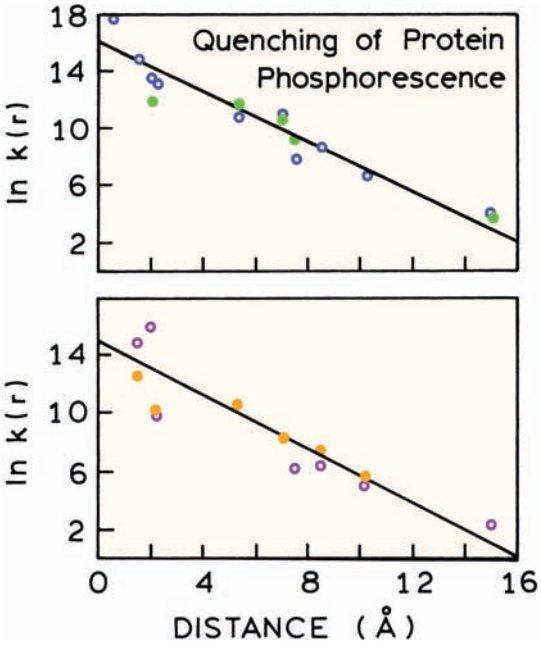

Figure 9.32. Relationship between Stern-Volmer quenching constants and distance from the protein surface. Top: quenching constants for nitrite (○) and azide (●). Bottom: quenching constants for ethanethiol (○) and nicotinamide (●). From [94].

by the RBC model. The data show a decrease in lifetime even in the absence of diffusion. This is not consistent with a sphere of action because the fluorophore–quencher pairs within the sphere are quenched and do not contribute to the intensity decay. Such data (Figure 9.31) can be explained by a short range exponential interaction.

9.6.2. Distance-Dependent Quenching in Proteins

The concept of distance-dependent quenching has been used to explain the quenching of protein phosphorescence by polar molecules (nitrite and azide), which were not expected to penetrate the proteins[94]. A number of single-tryptophan proteins were examined, for which the crystal structures were known. There was a strong correlation between the quenching constant and the distance of the tryptophan to the surface of the protein (Figure 9.32). The quenching constants were not sensitive to solution viscosity, suggesting that the rate of quenching was sensitive to the distance of closest approach. The exponential dependence of quenching constants on distance from the surface indicated that electron transfer or electron exchange governed the quenching process.

REFERENCES

1. Turro NJ. 1978. *Modern molecular photochemistry*. Benjamin/Cummings, Menlo Park, CA.
2. Kavarnos GJ. 1993. *Fundamentals of photoinduced electron transfer*. VCH Publishers, New York.
3. Kavarnos GJ, Turro NJ. 1986, Photosensitization by reversible electron transfer: theories, experimental evidence, and examples. *Chem Rev* **86**:401–449.
4. Eftink MR, Selva TJ, Wasylewski Z. 1987. Studies of the efficiency and mechanism of fluorescence quenching reactions using acrylamide and succinimide as quenchers. *Photochem Photobiol* **46**: 3–30.
5. Eftink MR. 1991. Fluorescence quenching: theory and applications. In *Topics in fluorescence spectroscopy*, Vol. 2: *Principles*, pp. 53–126. Ed JR Lakowicz. Plenum Press, New York.
6. Zhang J, Roek. DP, Chateauneuf JE, Brennecke JF. 1997. A steady-state and time-resolved fluorescence study of quenching reactions of anthracene and 1,2-benzanthracene by carbon tetrabromide and bromoethane in supercritical carbon dioxide. *J Am Chem Soc* **119**: 9980–9991.
7. Lessard G, Durocher G. 1978. Singlet and triplet quenching of indole by heavy atom containing molecules in a low temperature glassy matrix, evidence for complexation in the triplet state. *J Phys Chem* **82**:2812–2819.
8. Khwaja HA, Semeluk GP, Unger I. 1982. Quenching of the singlet and triplet state of benzene by hologenated alkanes in the vapor phase. *Can J Chem* **60**(13):1767–1774.
9. Berlman IB. 1973. Empirical study of heavy-atom collisional quenching of the fluorescence state of aromatic compounds in solution. *J Phys Chem* **77**(4):562–567.
10. Kasha M. 1952. Collisional perturbation of spin-orbital coupling and the mechanism of fluorescence quenching: a visual demonstration of the perturbations. *J Chem Phys* **20**(1):71–74.
11. DeToma RP, Cowan DO. 1975. External heavy-atom perturbed intersystem crossing from the excited singlet and triplet states of anthracene and 9,10-dibromoanthracene in fluid solution. *J Am Chem Soc* **97**(12):3283–3291.
12. Mac M. 1995. Fluorescence quenching of aromatic molecules by inorganic anions in polar solvents. *J Luminesc* **65**:143–151.
13. Kropp JL, Burton M. 1962. Effect of added quenchers in organic scintillator solutions: organometallics. *J Chem Phys* **37**(8): 1752–1756.
14. Dreeskamp H, Laufer A, Zander M. 1983. Quecheing of the perylene fluorescence by Ag^{+}-ions. *Z Naturforsch A* **38**:698–700.
15. Evans DF. 1957. Perturbation of singlet–triplet transitions of aromatic molecules by oxygen under pressure. *J Chem Soc*, 1351–1357.
16. Kawaoka K, Khan AU, Kearns DR. 1967. Role of singlet excited states of molecular oxygen in the quenching of organic triplet states. *J Chem Phys* **46**(5):1842–1853.
17. Kearns DR, Stone AJ. 1971. Excited-state intermolecular interactions involving paramagnetic molecules: effect of spin–spin and spin–orbit interactions on the quenching of triplets. *J Chem Phys* **55**(7):3383–3389.
18. Kikuchi K, Sato C, Watabe M, Ikeda H, Takahashi Y, Miyashi T. 1993. New aspects on fluorescence quenching by molecular oxygen. *J Am Chem Soc* **115**:5180–5184.

19. Parmenter CS, Rau JD. 1969. Fluorescence quenching in aromatic hydrocarbons by oxygen. *J Chem Phys* **51**(5):2242–2246.
20. Camyshan SV, Gritsan NP, Korolev VV, Bazhin NM. 1990. Quenching of the luminescence of organic compounds by oxygen in glassy matrices. *Chem Phys* **142**:59–68.
21. Alford PC, Cureton CG, Lampert RA, Phillips D. 1983. Fluorescence quenching of tertiary amines by halocarbons. *Chem Phys* **76**:103–109.
22. Najbar J, Mac M. 1991. Mechanisms of fluorescence quenching of aromatic molecules by potassium iodide and potassium bromide in methanol-ethanol solutions. *J Chem Soc Faraday Trans* **87**(10): 1523–1529.
23. Goswami D, Sarpal RS, Dogra SK. 1991. Fluorescence quenching of few aromatic amines by chlorinated methanes. *Chem Soc Jpn* **64**:3137–3141.
24. Bortolus P, Bartocci G, Mazzucato U. 1975. Excited state reactivity of aza aromatics, III: quenching of fluorescence and photoisomerization of azastilbenes by inorganic anions. *J Phys Chem* **79**:21–25.
25. Watkins AR. 1974. Kinetics of fluorescence quenching by inorganic anions. *J Phys Chem* **78**(25):2555–2558.
26. Carrigan S, Doucette S, Jones C, Marzzacco CJ, Halpern AM. 1996. The fluorescence quenching of 5,6-benzoquinoline and its conjugate acid by Cl^-, Br^-, SCN^- and I^- ions. *J Photochem Photobiol A: Chem* **99**:29–35.
27. Ahmad A, Durocher G. 1981. Fluorescence quenching of carbazole by holocarbons in 3-methylpentane solutions at room temperature. *Can J Spectrosc* **26**(1):19–24.
28. Ahmad A, Durocher G. 1981. How hydrogen bonding of carbazole to ethanol affects its fluorescence quenching rate by electron acceptor quencher molecules. *Photochem Photobiol* **34**:573–578.
29. Namiki A, Nakashima N, Yoshinara K. 1979. Fluorescence quenching due to the electron transfer: indole-chloromethanes in rigid ethanol glass. *J Chem Phys* **71**(2):925–932.
30. Tucker SA, Cretella LE, Waris R, Street KW, Acree WE, Fetzer JC. 1990. Polycyclic aromatic hydrocarbon solute probes, VI: effect of dissolved oxygen and halogenated solvents on the emission spectra of select probe molecules. *Appl Spectrosc* **44**:269–273.
31. Takahashi T, Kikuchi K, Kokubun H. 1980. Quenching of excited 2,5-diphenyloxazole by CCl_4. *J Photochem* **14**:67–76.
32. Ellison EH, Thoms JK. 2001. Photoinduced reaction of arene singlets with carbon tetrachloride in zeolite Y. *Microporous Mesoporous Mater* **49**(1–3):15-24.
33. Encinas MV, Rubio MA, Lissi EA. 1982. Quenching and photobleaching of excited polycyclic aromatic hydrocarbons by carbon tetrachloride. *J Photochem* **18**:137–150.
34. Dexter DL. 1953. A theory of sensitized luminescence in solids. *J Chem Phys* **21**(5):836–850.
35. Inokuti M, Hirayama F. 1965. Influence of energy transfer by the exchange mechanism on donor luminescence. *J Chem Phys* **43**(6): 1978–1989.
36. Kobayashi H, Morita T. 1973. Influence of triplet–triplet excitation transfer on the decay function of donor luminescence. *Chem Phys Lett* **20**(4):376–378.
37. Hasson S, Lustig H, Rubin. MB, Speiser S. 1984. The mechanism of short-range intramolecular electron energy transfer in bichromophoric molecules. *J Phys Chem* **88**:6367–6374.
38. Knibbe H, Rehm D, Weller A. 1968. Intermediates and kinetics of fluorescence quenching by electron transfer. *Ber Bunsenges* **72**(2): 257–263.
39. Kumbhakar M, Nath S, Rath MC, Mukherjee T, Pal H. 2004. Electron transfer interaction of dihydroxyquinones with amine quenchers: dependence of the quenching kinetics on the aliphatic and aromatic nature of the amine donors. *Photochem Photobiol* **74**(1): 1–10.
40. Rubstov IV, Shirota H, Yoshihara K. 1999. Ultrafast photoinduced solute–solvent electron transfer: configuration dependence. *J Phys Chem A* **103**:1801–1808.
41. Pal SK, Bhattacharya T, Misra T, Saini RD, Ganguly T. 2003. Photophysics of some disubstituted indoles and their involvements in photoinduced electron transfer reactions. *J Phys Chem A* **107**:10243–10249.
42. Jacques P, Haselbach E, Henseler A, Pilloud D, Suppan P. 1991. Multiple Rehm-Weller plots in the electron-transfer quenching of singlet excited 9,10-dicyanoanthracene. *J Chem Soc* **87**(24): 3811–3813.
43. Seidel CAM, Schulz A, Sauer MHM. 1996. Nucleobase-specific quenching of fluorescent dyes, 1: nucleobase one-electron redox potentials and their correlation with static and dynamic quenching efficiencies. *J Phys Chem* **100**:5541–5553.
44. Montejano HA, Cosa JJ, Garrera HA, Previtali CM, 1995. Solvent effects on the photoinduced electron transfer reaction between excited singlet pyrene and indole. *J Photochem Photobiol A: Chem* **86**:115–120.
45. Ghosh HN, Pal H, Palit DK, Mukherjee T, Mittal JP. 1993. Interaction of the excited singlet state of disubstituted anthraquinones with aliphatic and aromatic amines: a fluorescence quenching study. *J Photochem Photobiol A: Chem* **73**:17–22.
46. Cheung ST, Ware WR. 1983. Exciplex photophysics, 7: steric effects in exciplex photophysics. *J Phys Chem* **87**:466–473.
47. Zhou J, Shah RP, Findley BR, Braun CL. 2002. Long distance photoinduced electron transfer in solutions: a mechanism for producing large yields of free ions by electron transfer quenching. *J Phys Chem A* **106**:12–20.
48. Chang SLP, Schuster DI. 1987. Fluorescence quenching of 9,10-dicyanoanthracene by dienes and alkenes. *J Phys Chem* **91**:3644–3649.
49. Vos R, Engelborghs Y. 1994. A fluorescence study of tryptophan histidine interactions in the peptide anantin in solution. *Photochem Photobiol* **60**(1):24–32.
50. Ricci RW, Nesta JM. 1976. Inter- and intramolecular quenching of indole fluorescence by carbonyl compounds. *J Phys Chem* **80**(9): 974–980.
51. Evans RF, Kuntz RR, Volkert WA, Ghiron CA. 1978. Flash photolysis of *N*-acetyl-L-tryptophanamide: the relationship between radical yields and fluorescence quenching. *Photochem Photobiol* **27**: 511–515.
52. Suzki M, Sano M, Kimura M, Hanabusa K, Shirai H. 1999. Enhancement of quenching of polymer-bound ruthenium (II) complexes with MV^{2+} using L-tyrosine esters. *Eur Polym J* **35**:221–226.
53. Namiki A, Nakashima N, Yoshihara K. 1979. Fluorescence quenching due to the electron transfer: indole-chloromethanes in rigid ethanol glass. *J Chem Phys* **71**(2):925–930.

54. Nagai K, Tsukamoto J, Takamiya N, Kancko M. 1995. Effect of amino acid residue model on the photoinduced long-distance electron transfer from the excited $Ru(bpy)_3^{2+}$ to methylviologen in a polymer film. *J Phys Chem* **99**:6648–6651.
55. Pownall HJ, Smith LC. 1974. Fluorescence quenching of anthracene in charged micelles by pyridium and iodide ions. *Biochemistry* **13**(12):2594–2597.
56. Clayton AHA, Ghiggino KP, Wilson GJ, Keyte PJ, Paddon-Row MN. 1992. Photoinduced electron transfer in rigidly linked dimethoxynaphthalene-N-methylpyridinium donor–acceptor molecules. *Chem Phys Lett* **195**(2,3):249–254.
57. Johnson GE. 1980. Fluorescence quenching of carbazoles. *J Phys Chem* **84**:2940–2946.
58. Nad S, Pal H. 2000. Electron transfer from aromatic amines to excited coumarin dyes: fluorescence quenching and picosecond transient absorption studies. *J Phys Chem A* **104**:673–680.
59. Singh MK, Pal H, Sapre AV. 2000. Interaction of the excited singlet state of neutral red with aromatic amines. *Photochem Photobiol* **71**(3):300–306.
60. Nagasawa Y, Yartsev AP, Tominaga K, Johnson AE, Yoshibara K. 1993. Substituent effects on intermolecular electron transfer: coumarins in electron-donating solvents. *J Am Chem Soc* **115**:7922–7923.
61. Le TP, Rogers JE, Kelly LA. 2000. Photoinduced electron transfer in covalently linked 1,8-naphthalimide/viologen systems. *J Phys Chem A* **104**:6778–6785.
62. Vos R, Engelborghs Y. 1994. A fluorescence study of tryptophan-histidine interactions in the peptide anantin and in solution. *Photochem Photobiol* **60**(1):24–32.
63. Torimura M, Krata S, Yamada K, Yokomaku T, Kamagata Y, Kanagawa T, Kurane R. 2001. Fluorescence-quenching phenomenon by photoinduced electron transfer between a fluorescent dye and a nucleotide base. *Anal Sci* **17**:155–160.
64. Sauer M, Drexhage KH, Lieberwirth U, Muller R, Nord S, Zander C. 1998. Dynamics of the electron transfer reaction between an oxazine dye and DNA oligonucleotides monitored on the single-molecule level. *Chem Phys Lett* **284**:153–163.
65. Lewis FD, Wu T, Zhang Y, Letsinger RL, Greenfield SR, Wasielewski MR. 1997. Distance-dependent electron transfer in DNA hairpins. *Science* **277**:673–676.
66. Zang L, Liu R, Holman M, Nguyen KT, Adams DM. 2002. A single-molecule probe based on intramolecular electron transfer. *J Am Chem Soc* **124**:10640–10641.
67. Liu R, Holman M, Zang L, Adams DM. 2003. Single-molecule spectroscopy of intramolecular electron transfer in donor–bridge–acceptor systems. *J Phys Chem A* **107**:6522–6526.
68. Nemzek TL, Ware WR. 1975. Kinetics of diffusion-controlled reactions: transient effects in fluorescence quenching. *J Chem Phys* **62**(2):477–489.
69. Bamford CH, Tipper CFH, Compton RG. 1985 *Chemical kinetics*. Elsevier, New York.
70. Smoluchowski VM. 1916. Drei vortage über diffusion, brownsche molekularbewegung und koagulation von kolloidteilchen [Three lectures on diffusion, Brownian molecular motion and coagulation of colloids]. *Z Physik* **17**:557–571, 585–599. (An English translation is available in Chandrasekhar S, Kac M, Smoluchowski R. 1986. *Marian Smoluchowski, his life and scientific work*. Polish Scientific Publishers, Warsaw.)
71. Collins FC, Kimball GE. 1949. Diffusion-controlled reaction rates. *J Colloid Sci* **4**:425–437. (See also Collins FC. 1950. *J Colloid Sci* **5**:499–505 for correction.)
72. Yguerabide J, Dillon MA, Burton M. 1964. Kinetics of diffusion-controlled processes in liquids: theoretical consideration of luminescent systems—quenching and excitation transfer in collision. *J Chem Phys* **40**(10):3040–3052.
73. Ware WR, Novros JS. 1966. Kinetics of diffusion-controlled reactions: an experimental test of theory as applied to fluorescence quenching. *J Phys Chem* **70**:3246–3253.
74. Ware WR, Andre JC. 1980. The influence of diffusion on fluorescence quenching. In *Time-resolved fluorescence spectroscopy in biochemistry and biology*, pp. 363–392. Ed RB Cundall, RE Dale. Plenum Press, New York.
75. Lakowicz JR, Johnson ML, Gryczynski I, Joshi N, Laczko G. 1987. Transient effects in fluorescence quenching measured by 2-GHz frequency-domain fluorometry. *J Phys Chem* **91**:3277–3285.
76. Periasamy N, Doraiswamy S, Venkataraman B, Fleming GR. 1988. Diffusion controlled reactions: experimental verification of the time-dependent rate equation. *J Chem Phys* **89**(8):4799–4806.
77. Lakowicz JR, Kusba, J., Szmacinski H, Johnson ML, Gryczynski I. 1993. Distance-dependent fluorescence quenching observed by frequency-domain fluorometry. *Chem Phys Lett* **206**(5,6):455–463.
78. Lakowicz JR, Zelent B, Gryczynski I, Kusba J, Johnson ML. 1994. Distance-dependent fluorescence quenching of tryptophan by acrylamide. *Photochem Photobiol* **60**(3):205–214.
79. Naumann W. 2000. Reversible fluorescence quenching: generalized Stern-Volmer equations on the basis of self-consistent quenching constant relations. *J Chem Phys* **112**(16):7152–7157.
80. Zelent B, Kusba J, Gryczynski I, Johnson ML, Lakowicz JR. 1996. Distance-dependent fluorescence quenching of p-bis[2-(5-phenyloxazolyl)]benzene by various quenchers. *J Phys Chem* **100**:18592–18602.
81. Lakowicz JR, Zelent B, Kusba J, Gryczynski I. 1996. Distance-dependent quenching of nile blue fluorescence by N,N-diethylaniline observed by frequency-domain fluorometry. *J Fluoresc* **6**(4):187–194.
82. Naqvi KR, Martins J, Melo E. 2000. Recipes for analyzing diffusion-controlled reactions in two dimensions: time-resolved and steady-state measurements. *J Phys Chem B* **104**:12035–12038.
83. Kusba J, Lakowicz JR. 1994. Diffusion-modulated energy transfer and quenching: analysis by numerical integration of diffusion equation in Laplace space. *Methods Enzymol* **240**:216–262.
84. Novikov E, Molski A, Boens N. 2000. Identifiability of a model for diffusion-mediated intramolecular excited-state quenching. *J Chem Phys* **112**(12):5348–5352.
85. Gladkikh VS, Burshtein AI, Tavernier HL, Fayer MD. 2002. Influence of diffusion on the kinetics of donor–acceptor electron transfer monitored by the quenching of donor fluorescence. *J Phys Chem A* **106**:6982–6990.
86. Owen CS, Vanderkooi JM. 1991. Diffusion-dependent and -independent collisional quenching of fluorescence and phosphorescence. *Comments Mol Cell Biophys* **7**(4):235–257.

87. Klos J, Molski A. 2004. Global analysis of kinetic and stationary diffusion-mediated fluorescence quenching data. *J Phys Chem A* **108**:2370–2374.
88. Kusba J. 1998. Personal communication.
89. Zelent B, Gryczynski I, Kusba J, Johnson ML, Lakowicz JR. 1992. Distance-dependent fluorescence quenching of N-acetyl-L-tryptophanamide by acrylamide and iodide. *Proc SPIE* **2137**:412–424.
90. Lakowicz JR, Joshi NB, Johnson ML, Szmacinski H, Gryczynski I. 1987. Diffusion coefficients of quenchers in proteins from transient effects in the intensity decays. *J Biol Chem* **262**(23):10907–10910.
91. Eftink MR. 1990. Transient effects in the solute quenching of tryptophan residues in proteins. *SPIE Proc* **1204**:406–414.
92. Lakowicz JR, Kusba J, Szmacinski H, Johnson ML, Gryczynski I. 1993. Distance-dependent fluorescence quenching observed by frequency-domain fluorometry. *Chem Phys Lett* **206**(5,6):455–463.
93. Zelent B, Kusba J, Gryczynski I, Lakowicz JR. 1995. Distance-dependent quenching of anthracene fluorescence by N,N-diethylaniline observed by frequency-domain fluorometry. *Appl Spectrosc* **49**(1):43–50.
94. Vanderkooi JM, Englander SW, Papp S, Wright WW, Owen CS. 1990. Long-range electron exchange measured in proteins by quenching of tryptophan phosphorescence. *Proc Natl Acad Sci* **87**:5099–5103.

PROBLEMS

P9.1. *Calculation of an Oxidation Potential for a Fluorophore*: Figures 9.17 and 9.18 show that PET occurs from 1,8-naphthalimide to methylviologen. Calculate the maximum value of the reduction potential $E(D^+/D)$ for the fluorophore above which PET would not occur. The reduction potential of MV^{2+} is 0.4 V. The wavelength of the lowest electronic transition is 365 nm.

P9.2. Figure 9.33 shows emission spectra of two compounds. The short- and long-wavelength emissions are due to the fluorescence and phosphorescence of the dimethoxynaphthalene moiety. Explain the different fluorescence intensities of the two compounds.

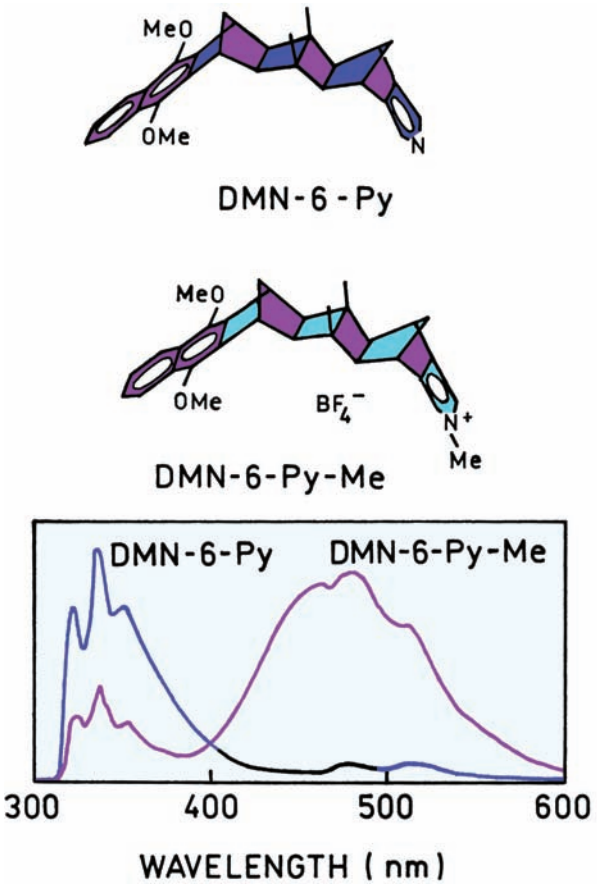

Figure 9.33. Emission spectra of DMN-6-Py and DMN-6-Py-Me in ethanol glass at 77°K. Revised from [56].